Wavelet Packet Division Multiplexing and Wavelet Packet Design Under Timing Error Effects

Kon Max Wong, *Senior Member, IEEE*, Jiangfeng Wu, Tim N. Davidson, *Member, IEEE*, and Qu (Gary) Jin

***Abstract*— Wavelet packet division multiplexing (WPDM) is a multiple signal transmission technique in which the message signals are waveform coded onto wavelet packet basis functions for transmission. The overlapping nature of such waveforms in time and frequency provides a capacity improvement over the commonly used frequency division multiplexing (FDM) and time division multiplexing (TDM) schemes while their orthogonality properties ensure that the overlapping message signals can be separated by a simple correlator receiver. The interference caused by timing offset in transmission is examined. A design procedure that exploits the inherent degrees of freedom in the WPDM structure to mitigate the effects of timing error is introduced, and a waveform that minimizes the energy of the timing error interference is designed. An expression for the probability of error due to the presence of Gaussian noise and timing error for the transmission of binary data is derived. The performance advantages of the designed waveform over standard wavelet packet basis functions are demonstrated by both analytical and simulation methods. The capacity improvement of WPDM, its simple implementation, and the possibility of having optimum waveform designs indicate that WPDM holds considerable promise as a multiple signal transmission technique.**

I. Introduction

WAVEFORM coding [1] is usually employed in a digital communication system to convert the message data into continuous waveforms in order to provide better immunity against noise, fading, or jamming during transmission. To achieve this aim, the various schemes of waveform coding endevor to make the distance between the waveforms in the coded signal as large as possible, i.e., to make the cross-correlation coefficient between any pair of waveforms as small as possible [2]. The smallest possible value of the cross-correlation coefficient is -1 when the waveforms are *antipodal*, with a distance of $2\sqrt{E}$ between its member waveforms (E being the waveform energy); however, this may only serve for a single binary signal. On the other hand, an *orthogonal* set of waveforms has all the cross-correlation coefficients equal to zero and has a distance equal to $\sqrt{2E}$ between its members. Compared with the antipodal case, the orthogonal waveforms may not provide as much immunity to noise and other interference, but a large number of independent massages, each having multilevel signaling, can be represented. Thus, orthogonal waveform coding remains widely used in communication systems.

To transmit a large number of independent messages over a common channel, two forms of orthogonality are commonly used [1], [3]–[5]: 1) orthogonality in frequency results in the method of *frequency division multiplexing* (FDM) in which bandlimited baseband digital signals are translated in frequency by modulating different sinusoidal carriers to occupy *nonoverlapping* bands, thereby partitioning the frequency bandwidth of the channel and allocating a different frequency band to each message signal; (2) orthogonality in time results in the method of *time division multiplexing* (TDM) in which the transmission of the message signals engages the channel periodically for different *nonoverlapping* time slots, thereby enabling the joint utilization of the channel by a plurality of message sources on a time-shared basis. FDM and TDM have been used to transmit multiuser communication signals for decades now and are the primary methods of multiplexing at present. However, waveform orthogonality is not limited to orthogonality in frequency or orthogonality in time only. It can be easily conceived that a set of waveforms that provides self-orthogonality based on translation in time and mutual orthogonality based on occupancy of different orthogonal subspaces can be utilized to code and multiplex the digital signals of a multiuser communication system. Wavelet and wavelet packet decompositions are convenient techniques (but by no means the only techniques) by which waveforms providing such orthogonalities can be obtained. Furthermore, such techniques can be easily implemented using multirate discrete-time filters. Several researchers have realized the potential of applying wavelets in multiuser communications, and various schemes of coding and multiplexing have been proposed [6]–[16]. In this paper, we study a multiplexing scheme employing the waveform coding ideas in [15]. We examine the performance of such a system from a transmission-reception point of view and propose an optimum orthogonal waveform set designed to minimize the errors induced by timing discrepancies.

First, let us briefly summarize the concepts of wavelets and multiresolution analysis, the details of which can be found in a number of textbooks [17]–[24] and tutorial articles [25]–[30]. A multiresolution analysis (MRA) [17], [31] consists of a

Manuscript received May 29, 1996; revised May 30, 1997. This work was performed while the authors were with the Communications Research Laboratory, McMaster University, Hamilton, Ont., Canada. The associate editor coordinating the review of this paper and approving it for publication was Dr. Guanghan Xu.

K. M. Wong is with the Department of Electronic Engineering, The Chinese University of Hong Kong, Shatin, Hong Kong, on leave from the Communications Research Laboratory, McMaster University, Hamilton, Ont., Canada L8S 4K1.

J. Wu is with Northern Telecom, Ottawa, Ont., Canada K1N 8T9.

T. N. Davidson is with the Communications Research Laboratory, McMaster University, Hamilton, Ont., Canada L8S 4K1.

Q. Jin is with Mitel Corporation, Kanata, Ont., Canada K2K 2A2.

Publisher Item Identifier S 1053-587X(97)08558-9.

collection of embedded subspaces[1]

$$\cdots \subset V_{21} \subset V_{11} \subset V_{01} \subset V_{-11} \subset \cdots \tag{1}$$

in the space of finite energy signals $\mathcal{L}_2(\mathcal{R})$ with some particular properties. Each subspace $V_{\ell 1}$ has an orthonormal basis $\{\phi_{\ell 1}(t - nT_\ell)\}_{n\in\mathcal{Z}}$, where $\mathcal{Z}$ represents the set of integers generated by translations of a single function. Furthermore, the basis functions for different subspaces can be obtained from each other by dyadic dilation, i.e.,

$$\phi_{\ell 1}(t) = 2^{\ell/2}\phi_{01}(2^{-\ell}t) \tag{2}$$

and $T_\ell = 2^\ell T_0$. Since $V_{\ell 1} \subset V_{\ell-1,1}$, we can write $\phi_{\ell 1}(t)$ as a linear combination of the orthonormal basis functions of $V_{\ell-1,1}$, i.e.,

$$\phi_{\ell 1}(t) = \sum_n h[n]\phi_{\ell-1,1}(t - nT_{\ell-1}) \tag{3}$$

where $h[n] = \langle \phi_{\ell-1,1}(t - nT_{\ell-1}), \phi_{\ell 1}(t)\rangle$ and $\langle\cdot,\cdot\rangle$ denotes the $\mathcal{L}_2$ inner product. A cursory examination of (2) and (3) reveals the close relation between $h[n]$ and $\phi_{\ell 1}(t)$, i.e.,

$$\phi_{\ell 1}(t) = \sqrt{2}\sum_n h[n]\phi_{\ell 1}(2t - nT_\ell). \tag{4}$$

Indeed, in order for the set of functions $\{\phi_{\ell 1}(t - nT_\ell)\}_{n\in\mathcal{Z}}$ to form an orthonormal basis for the space $V_{\ell 1}$, $h[n]$ must satisfy the orthonormality constraint

$$\sum_n h[n]h[n - 2m] = \delta[m] \tag{5}$$

where $\delta[m]$ is the Kronecker delta and some mild technical conditions [18], [32], including $\Sigma_n(-1)^n h[n] = 0$. Given such a sequence $h[n]$, we can find a sequence $g[n]$ satisfying $\Sigma_n\, g[n]h[n - 2m] = 0$ such that the function

$$\phi_{\ell 2}(t) = \sum_n g[n]\phi_{\ell-1,1}(t - nT_{\ell-1}) \tag{6}$$

forms an orthonormal basis for the orthogonal complement of $V_{\ell 1}$ in $V_{\ell-1,1}$, which we will denote by $V_{\ell 2}$. The sequence $g[n]$ can be chosen to be a reversed, modulated, and shifted version of $h[n]$

$$g[n] = (-1)^n h[2k + 1 - n]$$

where $k \in \mathcal{Z}$. The resulting basis functions $\phi_{\ell 1}(t)$ and $\phi_{\ell 2}(t)$ are called the *scaling function* and *wavelet at scale* ℓ, respectively. To interpret (3) and (6) in the familiar frequency domain, we note that $\phi_{\ell 1}(t)$ occupies only half the bandwidth of $\phi_{\ell-1,1}(t)$, due to their dilation relation. Thus, (3) and (6) can be conceived as a lowpass (LP) and a highpass (HP) discrete-time filtering (i.e., tapped delay line filtering [2], [33]) of the signal $\phi_{\ell-1,1}(t)$ to obtain $\phi_{\ell 1}(t)$ and $\phi_{\ell 2}(t)$, respectively. If the sequences $h[n]$ and $g[n]$ in a particular MRA are finite, they can be realized as finite impulse response (FIR) filters forming an orthonormal two-channel perfect reconstruction filter bank [18], [31], [32].

[1]Whilst the double subscript notation may seem redundant at this point, it simplifies the extension to wavelet packets.

In an analogous way to (3) and (6), we can recursively decompose the spaces $V_{\ell m}$ $(\ell \geq 0, 1 \leq m \leq 2^\ell)$ by partitioning the corresponding orthonormal bases $\{\phi_{\ell m}(t - nT_\ell)\}_{n\in\mathcal{Z}}$ in the following tree-structured manner [34]:

$$\phi_{\ell+1,2m-1}(t) = \sum_n h[n]\phi_{\ell m}(t - nT_\ell) \tag{7}$$

$$\phi_{\ell+1,2m}(t) = \sum_n g[n]\phi_{\ell m}(t - nT_\ell). \tag{8}$$

Here, the first subscript denotes the "level" in the tree structure induced by the recursive decomposition of V_{01}, and the second subscript denotes the position of a node in a given level. We can grow or prune the tree in any desired fashion, and the functions $\phi_{\ell m}(t)$ at the "leafs" or *terminals* of a given tree structure provide a set of "wavelet packet basis functions" or simply a *wavelet packet*, as exemplified in Fig. 1(a). The corresponding *subband* structure in the frequency domain is shown in Fig. 1(b). Since $V_{\ell+1,2m}$ is the orthogonal complement of $V_{\ell+1,2m-1}$ in $V_{\ell m}$, we can write the function $\phi_{\ell m}(t)$ as a linear combination of translated versions of $\phi_{\ell+1,2m-1}(t)$ and $\phi_{\ell+1,2m}(t)$. Using (7) and (8), the coefficients of the linear combination can be shown to be reversed versions of the decomposition sequences $h[n]$ and $g[n]$ (with appropriate upsampling) [31]. Continuing this process, we can reconstruct $\phi_{01}(t)$ from the terminal functions of an arbitrary tree-structured decomposition

$$\phi_{01}(t - nT_0) = \sum_{\ell\in\mathcal{L}, m\in\mathcal{M}_\ell} \sum_k f_{\ell m}[n - 2^\ell k]\phi_{\ell m}(t - kT_\ell)$$

where

- $\mathcal{L}$ set of levels containing the terminals of a given tree;
- $\mathcal{M}_\ell$ set of indices of the terminals at the ℓth level;
- $f_{\ell m}[n]$ equivalent sequence (filter) built from the combinations of $h[n], g[n]$ and dilation (downsampling), which lead from the root to the (ℓ, m)th terminal;

i.e.,

$$\phi_{\ell m}(t) = \sum_k f_{\ell m}[k]\phi_{01}(t - kT_0). \tag{9}$$

For a given tree structure, the functions $\phi_{\ell m}(t)$ in (9) will be called the *constituent terminal functions of* $\phi_{01}(t)$.

II. Application of Wavelet Packets in Multiple Signal Transmission

In our application of wavelet packets to multiple signal transmission, we consider a TDM system in which there are $K_{\ell m}$ independent binary message signals interlaced with each other. In between two consecutive binary symbols of the same message, there are $K_{\ell m} - 1$ other binary symbols: one from each of the other message signals. The combined sequence forms a composite sequence of binary symbols $\sigma_{\ell m}[n]$ such that $\sigma_{\ell m}[n] = \pm 1$. The system that we propose here seeks the representation of the binary symbols "1" and "−1" by $\phi_{\ell m}(t)$ and $-\phi_{\ell m}(t)$, respectively, so that the waveform coded

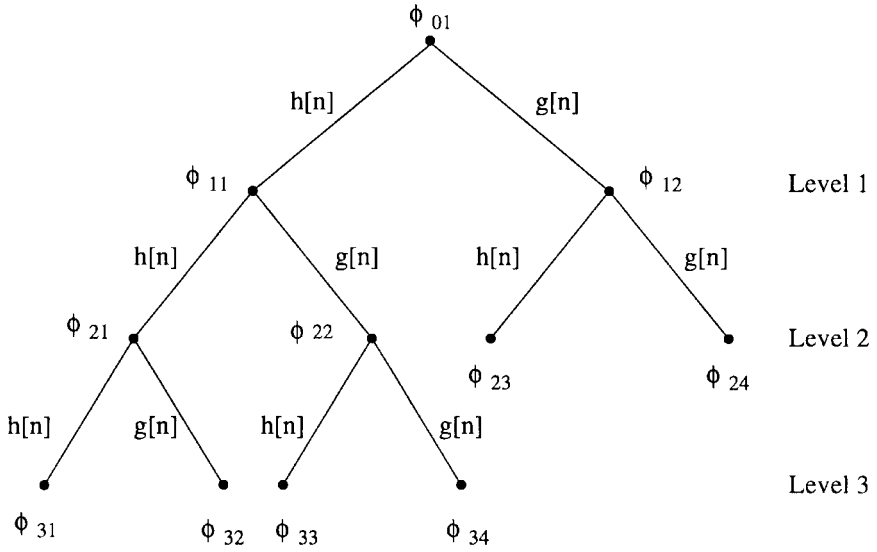

(a)

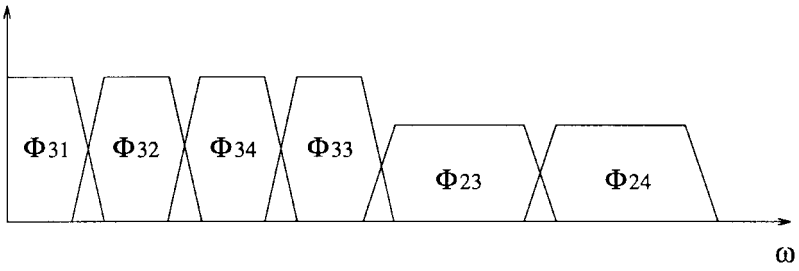

(b)

Fig. 1. (a) Typical WPDM tree structure. (b) Subband structure of the tree in part (a) for representative filters.

composite TDM sequence is given by

$$s_{\ell m}(t) = \sum_n \sigma_{\ell m}[n]\phi_{\ell m}(t - nT_\ell). \tag{10}$$

The optimal receiver for $s_{\ell m}(t)$ in the additive white Gaussian noise (AWGN) channel is the well-known correlator followed by a sampler [1], [3]–[5]. In practice, the scaling function $\phi_{01}(t)$ will usually be chosen to have finite duration so that the constituent terminal functions $\phi_{\ell m}(t)$ are also of finite duration (and the filters $h[n]$ and $g[n]$ are FIR filters). Note, however, that the duration of $\phi_{\ell m}(t)$ is often larger than the bit interval T_ℓ. The orthogonality of the set $\{\phi_{\ell m}(t - nT_\ell)\}_{n\in\mathcal{Z}}$ ensures that such overlap will not cause (intersymbol) interference.

Since all the constituent terminal functions in a given tree structure are orthogonal to each other, we may employ all of these functions to carry binary data from different TDM groups of users while maintaining the simple correlator structure of the receiver. The configuration of this multiple signal transmission system is shown in the left half of Fig. 2(a), in which the tree structure has been chosen to have M terminals. At the (ℓ, m)th terminal (the mth node of the ℓth level), the group of binary messages $\{r_1, \cdots, r_{K_{\ell m}}\}$ is time multiplexed by a commutator, and the resulting binary sequence $\sigma_{\ell m}[n]$ is waveform coded as in (10). Obviously, binary sequences waveform coded by constituent terminal functions at different levels will have different bit durations, whereas sequences at the same level have equal bit durations. At the output of the transmitter, we have a composite signal given by

$$s_c(t) = \sum_{\ell\in\mathcal{L}, m\in\mathcal{M}_\ell} \sum_n \sigma_{\ell m}[n]\phi_{\ell m}(t - nT_\ell). \tag{11}$$

The reception of such a composite signal can be carried out using a bank of correlating receivers, as shown on the right half of Fig. 2(a). However, by substituting (9) into (11), it can be seen that

$$\begin{aligned} s_c(t) &= \sum_{\ell\in\mathcal{L}, m\in\mathcal{M}_\ell} \sum_n \sigma_{\ell m}[n] \sum_k f_{\ell m}[k]\phi_{01}(t-(2^\ell n+k)T_0) \\ &= \sum_k \sigma_{01}[k]\phi_{01}(t-kT_0) \end{aligned} \tag{12}$$

where $\sigma_{01}[k]$ is the equivalent sequence at the root of the tree

$$\sigma_{01}[k] = \sum_{\ell\in\mathcal{L}, m\in\mathcal{M}} \sum_n f_{\ell m}[k - 2^\ell n]\sigma_{\ell m}[n] \tag{13}$$

from which the original message signals can be recovered using

$$\sigma_{\ell m}[n] = \sum_k f_{\ell m}[k - 2^\ell n]\sigma_{01}[k]. \tag{14}$$

Equations (12) and (13) suggest an alternative realization of the WPDM system in which the bank of modulators in the transmitter is replaced by a multirate filter bank built from filters with impulse responses $f_{\ell m}[-n]$ (or appropriately

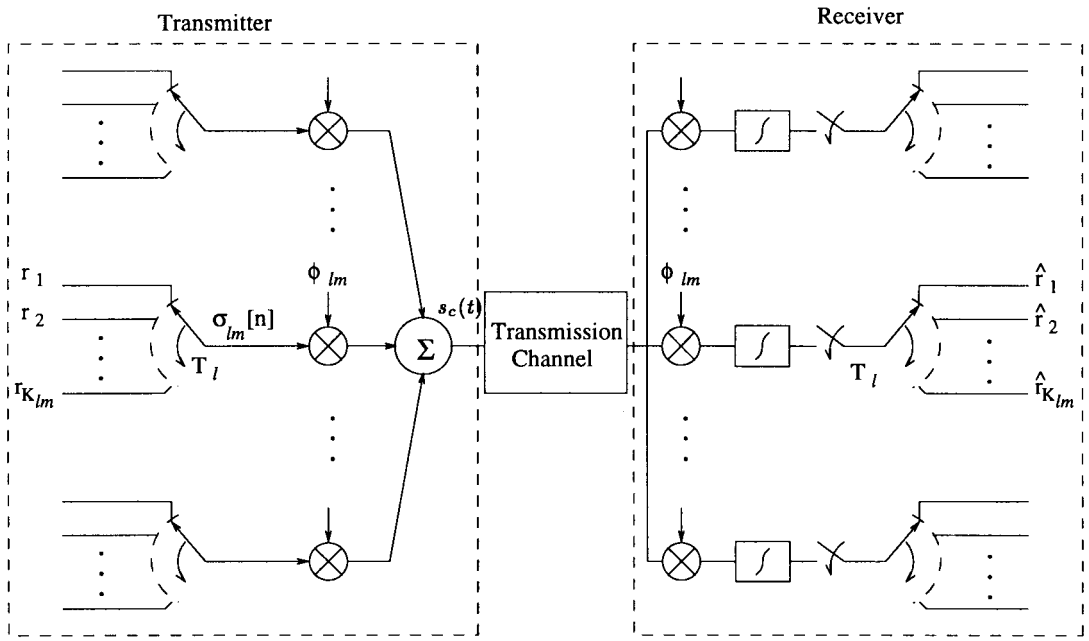

(a)

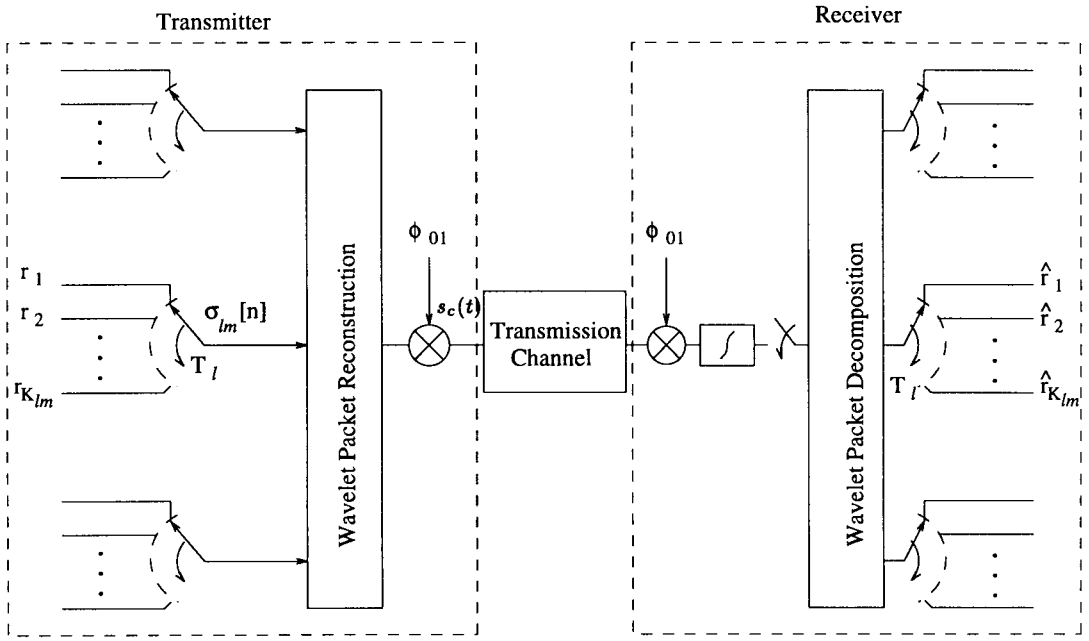

(b)

Fig. 2. Two equivalent transmission and reception systems for WPDM.

shifted versions thereof), which we will call a *wavelet packet reconstructor* and a single modulator. The receiver can also be alternatively realized, as suggested in (12) and (14), by a single correlator followed by a bank of discrete-time multirate filters with impulse responses $f_{\ell m}[n]$ that are called a *wavelet packet decomposer*. This equivalent configuration of the system is shown in Fig. 2(b).

We will call the multiple signal transmission and reception system in Fig. 2(a) and (b) wavelet packet division multiplexing (WPDM). It is noted that the transmitted signals in both realizations are identical and, hence, so is the performance of the systems in the AWGN channel. It is also noted that since the WPDM system transmits orthogonal antipodal waveforms to represent the binary data, its performance in the AWGN channel is identical to any other transmission system that uses such waveforms.

We can view the WPDM system as a combined form of TDM and FDM. If each user in a WPDM system is assigned a constituent terminal function $\phi_{\ell m}(t)$ to carry the message data, then the WPDM system is reduced to a wavelet carrier (WC) FDM system. On the other hand, if only $\phi_{01}(t)$ is employed to carry the time-multiplexed binary data from different users, then the WPDM system is reduced to a WC TDM system. It should be emphasized that the WC FDM and WC TDM

systems arrived at by taking the extreme cases of WPDM are different from conventional FDM and TDM systems in the sense that a conventional FDM/TDM system does not have overlapping frequency bands/time slots. However, in the special WC FDM/WC TDM systems, overlapping bands/slots are allowed. The signals from different users are separated by the orthogonality of the waveforms. The allowance of overlapping frequency bands/time slots results in an increase in the number of users being able to share the channel compared to FDM and TDM systems. This is shown as follows.

It is well known that both FDM and TDM systems as described in the Introduction require the same transmission bandwidth for a given number of users [1], [3]–[5]. Thus, it is sufficient to compare the required bandwidth of the WPDM system with that of the FDM system. We consider a multiuser communication system in which there are 2^ℓ user messages, each having a bit duration of T_ℓ seconds. In an FDM system transmitting such messages, the binary data of each message can be represented by rectangular pulses modulating a sinusoidal carrier. However, such representation occupies a large bandwidth. In practice, pulse shaping is performed so that the spectrum is bandlimited with a "raised cosine roll-off" spectral characteristic [1], [3]–[5]. The bandwidth required for each message is thus $(1+\alpha)/T_\ell$ Hz, where the roll-off factor α is chosen between 0 and 1. In addition, to avoid requiring very sharp cutoff characteristics in the channel filters separating the message signals from each other, the FDM system requires a guard band of bandwidth δ_g/T_ℓ between the frequency bands of each pair of adjacent message signals. Thus, the total bandwidth required by the FDM system is

$$W_F = \frac{2^\ell(1+\alpha+\delta_g)}{T_\ell} \text{ Hz.}$$

Now, consider the same 2^ℓ users employing the WPDM system in which each message modulates a finite duration constituent terminal function from the ℓth level of the tree structure in Fig. 2. Although the total bandwidth of the constituent terminal functions is theoretically infinite (the functions are of finite duration), we can define a γ-*effective bandwidth* of $\phi_{01}(t)$ to be β_γ/T_0 such that

$$\int_0^{2\pi\beta_\gamma/T_0} |\Phi_{01}(\omega)|^2\, d\omega = \gamma \int_0^{\infty} |\Phi_{01}(\omega)|^2\, d\omega \qquad (15)$$

where $\Phi_{01}(\omega)$ is the Fourier transform of $\phi_{01}(t)$ for $0<\gamma<1$. It is customary [35] to choose $\gamma = 0.99$. Of course, the γ-effective bandwidth in (15) is also the total γ-effective bandwidth of the 2^ℓ constituent terminal functions. For practical implementation, in order to avoid requiring sharp cutoff characteristics in the channel filters of the WPDM system, we transmit the 2^ℓ constituent terminal functions in double sideband (DSB). The total γ-effective bandwidth needed to transmit the 2^ℓ messages a practical WPDM system is

$$W_W = \frac{2\beta_\gamma}{T_0} = \frac{2^{\ell+1}\beta_\gamma}{T_\ell} \text{ Hz.}$$

TABLE I
VALUES OF β_γ AND η FOR SCALING FUNCTIONS GENERATED BY DAUBECHIES FILTERS OF LENGTH N WITH $\alpha = 0.5, \delta_g = 0.2$ AND $\gamma = 0.99$

N	4	6	8	10	12	14	16	18	20
β_γ	1.62	0.77	0.66	0.63	0.62	0.60	0.60	0.59	0.58
η	1.91	0.91	0.78	0.75	0.72	0.70	0.70	0.69	0.68

Hence, the ratio of the total bandwidths of the two systems is given by

$$\eta = \frac{W_W}{W_F} = \frac{2\beta_\gamma}{1+\alpha+\delta_g}.$$

There are many orthogonal scaling functions for which $\beta_\gamma<1$, among them, the well-known functions generated by Daubechies filters [18], [32] of length greater than or equal to 6. If we choose one for which the ratio $\eta<1$, we obtain a bandwidth reduction over the FDM (or TDM) system. Table I shows the values of β_γ for the Daubechies filters of different lengths, as well as the values of the bandwidth ratio η for the representative values $\alpha = 0.5$ and $\delta_g = 0.2$. It can be observed from the table that if a Daubechies filter of length 14 is used, the WPDM system requires only 70% of the transmission bandwidth required by the corresponding FDM system. The spectral energy characteristics of the two systems in the case of four users are illustrated in Fig. 3. Fig. 3(a) shows the characteristics of the four user messages in the FDM scheme, and Fig. 3(b) shows the characteristics of the same four user messages in the WPDM scheme (using Daubechies filters of length 14) transmitted in DSB. The combined frequency characteristic is shown by the solid line and the 99% energy bandwidth is also indicated. In closing this argument, we point out that the nature of the bandwidth saving discussed above is independent of the structure of the WPDM tree.

III. INTERFERENCE IN TRANSMISSION

The proposed multiple signal transmission and reception system [Fig. 2(a) or (b)] exploits the self- and mutual-orthogonality of the constituent terminal functions so that the message bits can be separated by a synchronous correlator. Signal transmission schemes based on synchronous correlators are vulnerable to errors caused by timing discrepancy; therefore, in this section, we analyze the effects of timing errors in the absence of channel noise. (Noise effects will be considered in Section V.) We consider the effects of *symbol synchronization* [36] error, which in the context of WPDM is the error that arises when the reference waveform generated at the receiver is not synchronized with the transmitted one. In the analysis in this section, we make the following assumptions.

1) Additive noise in the transmission channel is negligible.
2) The bandwidth of the communication channel is sufficiently large to not cause any significant distortion of the waveform of the transmitted signal.
3) Although the timing discrepancy Δ is, in general, a random variable, we assume that it is changing slowly so that over the transmission of a group of symbols, it can be regarded to be a constant error.

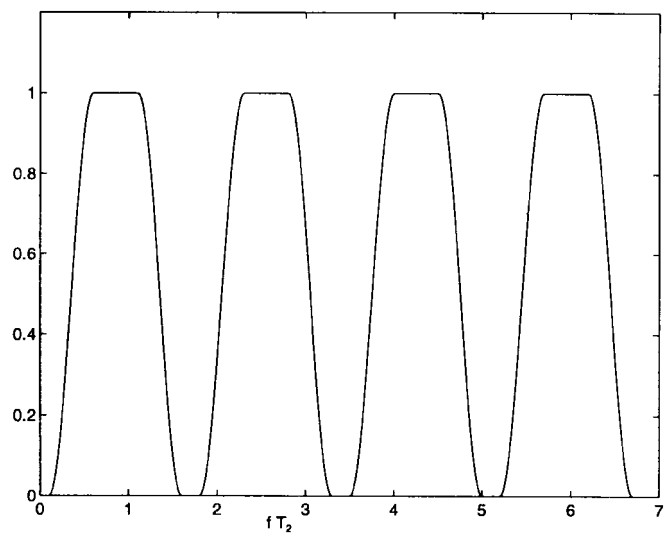

(a)

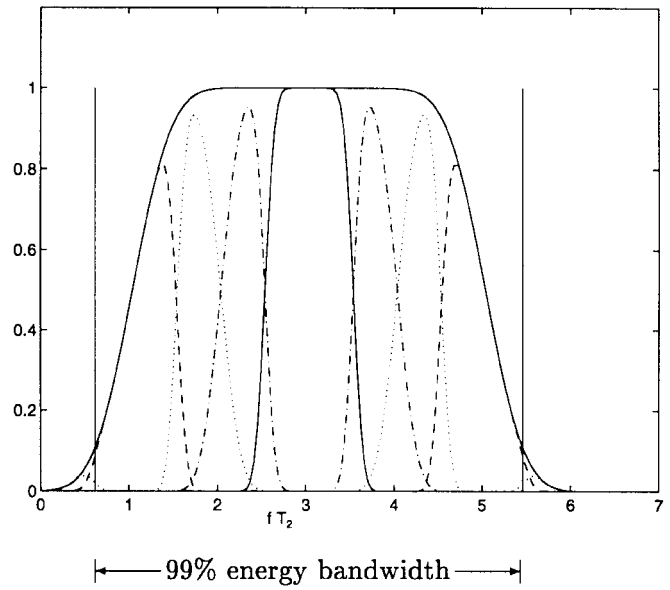

(b)

Fig. 3. Spectral energy characteristics of a four user system with frequency normalized to the bit rate $1/T_2$.

A straightforward analysis shows that under Assumption 3 above, the demodulated data at the (ℓ, m)th terminal in each of the receiver realizations in Fig. 2 are identical. Thus, we may use either of them to analyze the performance of the WPDM system under the effects of timing discrepancy. Here, we analyze the realization shown in Fig. 2(b), for which the transmitted signal $s_c(t)$ is given by (12). Let Δ denote the timing discrepancy between the transmitter and the receiver. In an attempt to recover the transmitted signal, the output of the correlator in the receiver is given by

$$\begin{aligned}\hat{\sigma}_{01}[n] &= \sum_k \sigma_{01}[k] \int \phi_{01}(t - kT_0)\phi_{01}(t - nT_0 + \Delta)\, dt \\ &= \sum_k \sigma_{01}[k] R_\phi(kT_0 - nT_0 + \Delta) \end{aligned} \tag{16}$$

where $R_\phi(\tau)$ is the autocorrelation function of $\phi_{01}(t)$. We assume that $\phi_{01}(t)$ is chosen in such a way (see also Proposition 2 in Section IV) that R_ϕ is differentiable. Hence, we can employ Taylor's formula with remainder [37] on (16), giving

$$\hat{\sigma}_{01}[n] = \sigma_{01}[n] + \Delta \sum_k \sigma_{01}[k] R'_\phi(kT_0 - nT_0) + O(\Delta^2) \tag{17}$$

where $R'_\phi(kT_0 - nT_0)$ denotes the derivative of $R_\phi(\tau)$ with respect to τ evaluated at $\tau = kT_0 - nT_0$, and the equality $R_\phi(kT_0 - nT_0) = \delta[k-n]$ has been used. Ignoring the terms involving second and higher orders of Δ, we can regard the second term on the right-hand side of (17) as the timing-discrepancy interference. Using the fact that $R_\phi(\tau)$ is an even function, we can rewrite this interference term as

$$I_{01}[n] = \Delta \sum_k (\sigma_{01}[n+k] - \sigma_{01}[n-k]) R'_\phi(kT_0). \tag{18}$$

After the correlator, the recovery of the estimates of the message signals $\hat{\sigma}_{\ell m}[n]$ requires the passing of $\hat{\sigma}_{01}[n]$ through the appropriate path of the wavelet packet decomposer given in (14). The interference at the (ℓ, m)th terminal is simply $I_{01}[n]$ passed through the same path of the decomposer, i.e.,

$$I_{\ell m}[n] = \sum_k f_{\ell m}[k - 2^\ell n] I_{01}[k] \tag{19}$$

$$\begin{aligned} &= \Delta \sum_k \sum_i (\sigma_{01}[k+i] - \sigma_{01}[k-i]) \\ &\quad \cdot R'_\phi(iT_0) f_{\ell m}[k - 2^\ell n]. \end{aligned} \tag{20}$$

Substituting (13) into (20), we have

$$\begin{aligned} I_{\ell m}[n] = \Delta &\sum_{\lambda \in \mathcal{L}, \mu \in \mathcal{M}_\lambda} \sum_j \sigma_{\lambda\mu}[j] \sum_i R'_\phi(iT_0) \\ &\times \sum_k f_{\lambda\mu}[k + i - 2^\lambda j] f_{\ell m}[k - 2^\ell n] \\ &- f_{\lambda\mu}[k - i - 2^\lambda j] f_{\ell m}[k - 2^\ell n]. \end{aligned}$$

To simplify the notation, we define the cross-correlation sequences

$$C^{\lambda\mu}_{\ell m}[n] = \sum_k f_{\lambda\mu}[k+n] f_{\ell m}[k] \tag{21}$$

and the coefficients

$$J^{\lambda\mu}_{\ell m}[n] = \sum_i R'_\phi(iT_0)(C^{\lambda\mu}_{\ell m}[n+i] - C^{\lambda\mu}_{\ell m}[n-i]). \tag{22}$$

This allows us to express the interference at the (ℓ, m)th terminal as

$$\begin{aligned} I_{\ell m}[n] &= \Delta \sum_{\lambda \in \mathcal{L}, \mu \in \mathcal{M}_\lambda} \sum_j \sigma_{\lambda\mu}[j] \sum_i R'_\phi(iT_0) \\ &\quad \cdot (C^{\lambda\mu}_{\ell m}[i - 2^\lambda j + 2^\ell n] - C^{\lambda\mu}_{\ell m}[2^\ell n - i - 2^\lambda j]) \\ &= \Delta \sum_{\lambda \in \mathcal{L}, \mu \in \mathcal{M}_\lambda} \sum_j \sigma_{\lambda\mu}[j] J^{\lambda\mu}_{\ell m}[2^\ell n - 2^\lambda j]. \end{aligned} \tag{23}$$

We can interpret (23) as follows. The interference at the (ℓ, m)th terminal is the sum of multirate filtered versions of the constituent sequences $\sigma_{\lambda\mu}[n]$ from each of the terminals. The filtering process consists of upsampling by 2^λ, filtering with impulse response $J^{\lambda\mu}_{\ell m}[n]$, and then downsampling by 2^ℓ.

We will therefore refer to a set of coefficients $J_{\ell m}^{\lambda\mu}[n]$ as an interference filter. As expected, the interference due to timing discrepancy arises not only from message signals using the same constituent terminal function (intersymbol interference) but also from message signals using other constituent terminal functions as waveforms (crosstalk). If the user message bits are independent, then using (23), the variance of the interference at the (ℓ, m)th terminal can be shown to be directly proportional to the sum of $\Sigma_n |J_{\ell m}^{\lambda\mu}[n]|^2$ over all relevant λ and μ.

An important observation is that the total energy of the interference at the terminals is independent of the tree structure. We formalize this as the following proposition [19], [23].

Proposition 1: The total energy of the interference at the terminals of a WPDM system due to timing discrepancy is independent of the tree structure, i.e.,

$$\sum_n |I_{01}[n]|^2 = \sum_{\ell\in\mathcal{L}, m\in\mathcal{M}_\ell} \sum_n |I_{\ell m}[n]|^2.$$

This energy balance between the initial and decomposed interferences is a direct result of Parseval's theorem. The wavelet packet decomposition is an orthonormal transformation, and hence, the norm is preserved.

Proposition 1 has a far-reaching implication: If our sole objective is to reduce the total energy of the timing-discrepancy interference, then regardless of the tree structure of the WPDM system, we can achieve this by choosing a $\phi_{01}(t)$ so that the energy of I_{01} is minimized. In the next section, we will design an optimal $\phi_{01}(t)$ based on the minimization of the total interference energy. However, it is observed from (19) that the interference at a particular terminal depends on both $\phi_{01}(t)$ and the position of that terminal in the tree. Thus, although the total energy of the interference remains independent of the tree structure, the distribution of the interference energy to different terminals is dependent on the structure.

IV. Optimum Wavelet Design

From the discussion in Section III, we can see that timing discrepancy in the WPDM system gives rise to interference in the forms of intersymbol interference and crosstalk. Various standard techniques, such as adaptive equalization [1], [3]–[5], may be used to reduce this interference, but in WPDM, we have an extra degree of freedom: the design of the waveform $\phi_{01}(t)$. Once the scaling function $\phi_{01}(t)$ is determined, all the constituent terminal functions to be used as waveforms are also determined by (7) and (8). Hence, we need only to design $\phi_{01}(t)$. If we design $\phi_{01}(t)$ to minimize the energy of the timing-discrepancy interference at the root of the WPDM tree, such a function also minimizes the total interference energy, regardless of the wavelet packet tree structure (Proposition 1).

In order to formulate the optimization problem, recall that $\phi_{01}(t)$ is intimately related to the filter coefficients $h[n]$ via the dilation equation of (4). In practical implementations of a WPDM system, we prefer $\phi_{01}(t)$ to be of finite duration, which implies that $h[n]$ is an FIR filter [18], [32]. Once the filter coefficients $h[n]$ are specified, the scaling function $\phi_{01}(t)$ can be obtained using any one of a number of possible algorithms [18], [25], [26], [32]. Now, using (18), we see that if the message bits are independent, the variance of the interference at the root of the tree is directly proportional to $\Sigma_n |R'_\phi(nT_0)|^2$. In addition, $R'_\phi(nT_0)$ can be calculated directly from the set of filter coefficients $\{h[n]\}$ using the following simple formulae [38]:

$$\begin{aligned} R'_\phi(nT_0) = 2R'_\phi(2nT_0) + 2\sum_{k=1}^{N/2} \rho_h[2k-1] \\ \cdot (R'_\phi((2n-2k+1)T_0) \\ + R'_\phi((2n+2k-1)T_0)) \end{aligned} \tag{24}$$

and

$$\sum_k kR'_\phi(kT_0) = -1 \tag{25}$$

where N is the length of the filter $h[n]$, and $\rho_h[k] = \Sigma_{n=0}^{N-k-1} h[n]h[n+k]$ is the autocorrelation sequence for $h[n]$. Thus, the problem is reduced to the design of a sequence $h[n]$ to minimize the objective functional

$$F = \sum_n |R'_\phi(nT_0)|^2. \tag{26}$$

The domain of $h[n]$ in the minimization of F must be constrained so that $h[n]$ satisfies the orthonormality condition of (5), which is rewritten here as

$$\sum_{n=2k}^{N-1} h[n]h[n-2k] - \delta[k] = 0, \qquad k = 0, 1, \cdots, N/2-1 \tag{27}$$

for which a necessary condition is that N is even [39]. In addition, to ensure that the locally linear approximation of (17) holds, $R_\phi(\tau)$ must be differentiable. For FIR filters, the differentiability constraint on $R_\phi(\tau)$ is satisfied if we choose a filter satisfying the following "regularity condition" with $K_0 \geq 1$.

Proposition 2: Let $h[n]$ be a sequence of length N starting at $n = 0$ that satisfies the orthogonality constraint in (27) and has a Z-transform of the form

$$H(z) = \sqrt{2}\left(\frac{1+z^{-1}}{2}\right)^K P(z) \tag{28}$$

where $1 \leq K \leq N/2$, and $P(z)$ is a polynomial in z^{-1} of degree $N-K-1$ with $|P(1)| = 1$. If $P(z)$ is bounded such that

$$|P(e^{j\omega})| < B, \quad \text{for all } \omega \in [0, \pi] \tag{29}$$

then $R_\phi(\tau)$ has (at least) $K_0 = 2K - 1 - \lceil 2 \log_2 B \rceil$ continuous derivatives, where $\lceil x \rceil$ denotes the least integer $\geq x$.

Using the fact that the Fourier transform of $R_\phi(\tau)$ is equal to $|\Phi_{01}(\omega)|^2$, where $\Phi_{01}(\omega)$ is the Fourier transform of $\phi_{01}(t)$, the proof of Proposition 2 follows the same line of argument as that of the (regularity) condition for $\phi_{01}(t)$ to have continuous derivatives [32]. The details of the proof can be found in [40]. For given N and K, the factorization of (28) can be ensured by having [41]

$$\sum_{n=0}^{N-1} (-1)^n n^k h[n] = 0, \qquad k = 0, 1, \cdots, K-1 \tag{30}$$

TABLE II
COEFFICIENTS OF THE OPTIMUM FILTER $\tilde{h}$ IN EXAMPLE 1

$\tilde{h}[0]$	$\tilde{h}[1]$	$\tilde{h}[2]$	$\tilde{h}[3]$	$\tilde{h}[4]$	$\tilde{h}[5]$	$\tilde{h}[6]$
0.021474	0.061336	0.144399	0.269674	0.427230	0.513130	0.364040

$\tilde{h}[7]$	$\tilde{h}[8]$	$\tilde{h}[9]$	$\tilde{h}[10]$	$\tilde{h}[11]$	$\tilde{h}[12]$	$\tilde{h}[13]$
-0.090059	-0.463195	-0.042816	0.299628	-0.034431	-0.086486	0.030273

and for a given B, since $|H(e^{j\omega_i})| = |\Sigma_{n=0}^{N-1} h[n]e^{-j\omega_i}|$, the frequency response bound of (29) can be enforced by requiring that

$$\left|\sum_{n=0}^{N-1} h[n]e^{-j\omega_i}\right| - 2^{-K+1/2}|(1+e^{j\omega_i})^K|(B-\epsilon) < 0 \quad (31)$$

for a suitable set of $\omega_i \in [0,\pi]$ (referred to here as the constraint frequencies) and an appropriate small positive number ϵ. In formulating the constraint in (31), we have exploited the fact that $H(z)$ is a polynomial in z^{-1} (it is an FIR filter) and, hence, cannot contain singularities on the unit circle. This ensures that for an appropriate set of constraint frequencies and an appropriate ϵ, the frequency response bound in (31) is not broken between the constraint frequencies. The minimization of F in (26) together with the constraints of (27), (30), and (31) can then be carried out by the Lagrange multiplier method.

From the above discussion, the procedure for the design of a scaling function $\phi_{01}(t)$ for WPDM that minimizes the total energy of the timing error interference can be summarized as follows.

1) Choose N (even), which is the length of the FIR filter $H(z)$. Choose K $(1 \le K \le N/2)$, which is the number of zeros of $H(z)$ at $z = -1$, and $B > 1$ such that $K_0 = 2K - 1 - \lceil 2 \log_2 B \rceil \ge 1$, which is the number of continuous derivatives of $R_\phi(\tau)$, satisfies $K_0 \ge 1$.
2) For a set of filter coefficients $h[n], n = 0, \cdots, N-1$, $R'_\phi(nT_0)$ can be calculated using (24) and (25), and thus, the cost functional F of (26) can be evaluated.
3) A new functional G, which is the sum of F and the $(N/2 + K)$ equality constraints of (27) and (30) and the inequality constraints of (31) multiplied by their corresponding Lagrange multipliers, can then be formed.
4) Employ an iterative numerical technique, e.g., sequential quadratic programming [42], to find a stationary point of G and, hence, obtain the optimum set of filter coefficients $\tilde{h}[n]$.
5) The optimum scaling function $\tilde{\phi}_{01}(t)$ can then be obtained by a recursive algorithm [18], [25], [26], [32].

In this paper, Step 5 is carried out using the "cascade" algorithm [32] in which the approximations are successively refined by dyadic contraction and filtering with the optimum filter coefficients $\tilde{h}[n]$ starting with a unit energy "box" function of duration T_0. That is,

$$\tilde{\phi}_{01}^{(j)}(t) = \sqrt{2}\sum_n \tilde{h}[n]\tilde{\phi}_{01}^{(j-1)}(2t - nT_0) \quad (32)$$

where $\tilde{\phi}_{01}^{(j)}$ is the jth approximation of the optimum $\tilde{\phi}_{01}(t)$, and

$$\tilde{\phi}_{01}^{(0)}(t) = \begin{cases} 1/\sqrt{T_0} & 0 \le t < T_0 \\ 0 & \text{otherwise.} \end{cases}$$

We terminated the iteration of the approximation when $\|\tilde{\phi}_{01}^{(j)}(t) - \tilde{\phi}_{01}^{(j-1)}(t)\|_2 \le \epsilon_\phi$, where $\|\cdot\|_2$ denotes the $\mathcal{L}_2$ norm, and ϵ_ϕ is a preset accuracy measure.

We employ the above procedure to design an optimum scaling function for the WPDM system in the following example.

Example 1: In this example, we show how a scaling function $\phi_{01}(t)$ can be designed to minimize the total interference energy due to timing discrepancy in the WPDM system. For the design, we chose $N = 14, K = 2$ and $B = \sqrt{2}$ so that $R_\phi(\tau)$ was guaranteed to be differentiable. A procedure based on the steps outlined above was employed to obtain the optimum filter coefficients $\{h[n]; n = 0, 1, \cdots, 13\}$ subject to the orthonormality and regularity constraints. The values of these optimal coefficients are shown in Table II. The optimum scaling function $\tilde{\phi}_{01}(t)$ was then obtained from the set of filter coefficients by the "cascade" algorithm given by (32), which generates an approximation to the optimum $\tilde{\phi}_{01}(t)$ "off-line," as shown in Fig. 4(a). Its autocorrelation function is shown in Fig. 4(b). Once the numerical values of (the approximation to) $\tilde{\phi}_{01}(t)$ have been obtained using (32), the scaling function can be generated "on-line" by standard pulse shaping techniques, the most commonly used being the employment of a tapped-delay line (transversal) filter followed by a smoothing filter [43]–[45].

Table III (last column) shows the comparison of the total interference due to timing error at the two terminals of the first level of the WPDM tree. The comparison is between the optimum scaling function $(N = 14)$ and two other scaling functions that have been widely used in other signal processing applications—the function generated by the Daubechies filter of length $N = 14$ [18], [32] and the Lemarié–Battle scaling function based on cubic splines [46], [47] (which are approximated by finite-duration function of length $31T_0$). It can be observed from Table III that the use of the optimum scaling function yields the smallest amount of interference due to timing error. To illustrate the distribution of the interference energy, we also show in the first four columns of Table III the values of the intersymbol interference energies $\Sigma_n|J_{11}^{12}[n]|^2$ and $\Sigma_n|J_{12}^{12}[n]|^2$ at the first and second terminals of the first level of the WPDM tree, as well as the respective crosstalk terms $\Sigma_n|J_{11}^{12}[n]|^2$ and $\Sigma_n|J_{12}^{11}[n]|^2$.

It should be noted that the mapping from signal waveform to energy is many to one, and therefore, $\tilde{\phi}_{01}(t)$ is not unique. A

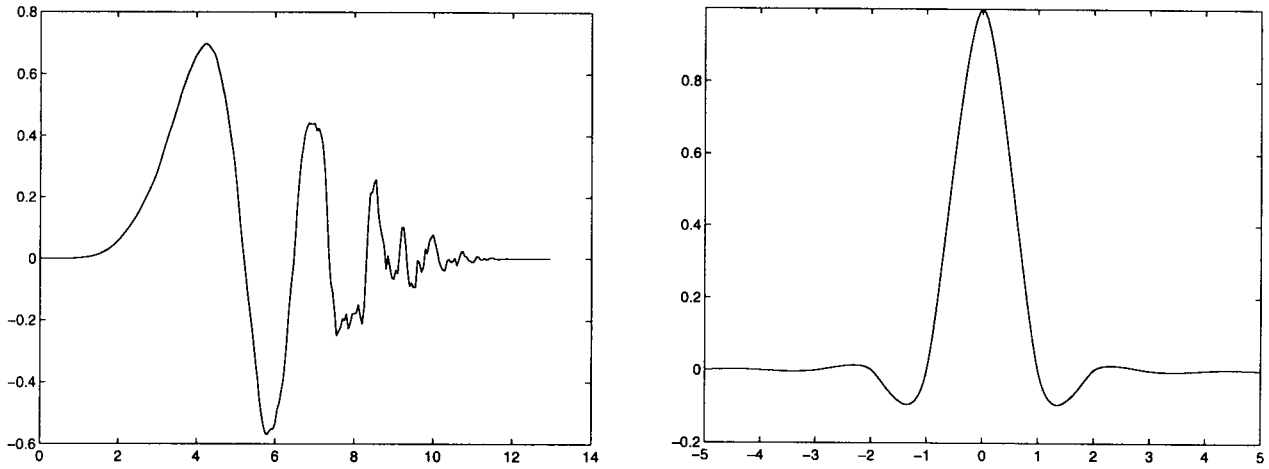

(a) (b)

Fig. 4. Optimum scaling function $\tilde{\phi}_{01}(t)$ from Example 1 and its autocorrelation function.

TABLE III
INTERFERENCE ENERGIES FOR SEVERAL SCALING FUNCTIONS FROM EXAMPLE 1

	$\sum \lvert J_{11}^{11}\rvert^2$	$\sum \lvert J_{11}^{12}\rvert^2$	$\sum \lvert J_{12}^{11}\rvert^2$	$\sum \lvert J_{12}^{12}\rvert^2$	total
optimum	0.261	0.542	0.542	0.742	2.086
Daubechies	0.422	0.464	0.464	2.024	3.374
Lemarié-Battle	0.548	0.304	0.304	3.228	4.384

different initial point in the optimization may lead to a different optimum $\tilde{\phi}_{01}(t)$, which also minimizes the interference energy.

V. BIT ERROR RATE

We now turn to the derivation of the probability of error in the reception of the binary messages under the influence of timing error interference. We examine the case where the channel is corrupted by stationary zero-mean additive white Gaussian noise (AWGN) $\nu(t)$ using the equivalent realization of Fig. 2(a). Since the timing error interference at a particular terminal depends on the position of the terminal in the WPDM tree structure, as seen in (19), the probability of error at each terminal is structure dependent. The binary message signal $\sigma_{\ell m}[n]$ at the (ℓ, m)th terminal, which takes on one of two possible values ± 1 is carried across the channel by the constituent terminal function $\phi_{\ell m}(t - nT_\ell)$ and is recovered by the correlator and sampler at the receiver. A consequence of the orthogonality properties of the constituent terminal functions is that the output of the (ℓ, m)th correlator, in the absence of noise and timing error, is simply

$$\hat{\sigma}_{\ell m}[n] = \int \sigma_{\ell m}[n]\phi_{\ell m}^2(t - nT_\ell)\, dt = \begin{cases} 1 & \text{if a "1" is sent} \\ -1 & \text{if a "}-1\text{" is sent.} \end{cases}$$

Therefore, assuming equal probabilities of ± 1, the optimal decision threshold is at zero. To incorporate the effects of timing error interference, recall from (23) that the interference at the (ℓ, m)th terminal is the sum of multirate filtered versions of the message signals from each terminal. For each instant n, the message bit $\sigma_{\ell m}[n]$ can be modeled as a random variable that takes on the values $+1$ and -1 with equal probabilities. In order to determine the probability distribution of the resulting interference, we must determine how many message bits contribute to the interference. To this end, we note that if the filter $h[n]$ is of length N, the length of the equivalent filter from the root of the tree to the (ℓ, m)th terminal $f_{\ell m}[n]$ is $N_\ell = (2^\ell - 1)(N - 1) + 1$, [23]. Using (21) and (22) and the fact that $R_\phi(\tau)$ is zero outside $(-(N-1)T_0, (N-1)T_0)$, the interference filter $J_{\ell m}^{\lambda\mu}[n]$ is zero outside an interval of length

$$N_\ell^\lambda = (2^\ell + 2^\lambda)(N - 1) - 1.$$

This means that from the (λ, μ)th terminal to the (ℓ, m)th terminal, there is a linear combination of N_ℓ^λ binary random variables, yielding a total of $2^{(N_\ell^\lambda)}$ discrete values. Another terminal at the level λ will contribute another $2^{(N_\ell^\lambda)}$ possible discrete values. Thus, the total number of possible discrete values of interference at the (ℓ, m)th terminal is given by

$$L_{\ell m} = \prod_{\lambda \in \mathcal{L}} 2^{M_\lambda (N_\ell^\lambda)}$$

where M_λ is the number of terminals at level λ. The magnitudes of these discrete interference values depend on the coefficients of the interference filters (23) but because $\sigma_{\lambda\mu}[n]$ takes on values of ± 1 with equal probabilities, these discrete interference values are equally likely and are symmetrically distributed about zero. If we denote the total interference due to timing discrepancy at the (ℓ, m)th terminal by the random variable $u_{\ell m}$, then its probability density function (PDF) is given by

$$p(u_{\ell m}) = \frac{1}{L_{\ell m}} \sum_{i=1}^{L_{\ell m}} \delta(u_{\ell m} - I_{\ell m;i}) \tag{33}$$

where $\delta(\cdot)$ denotes the Dirac delta function, and $I_{\ell m;i}$ denotes

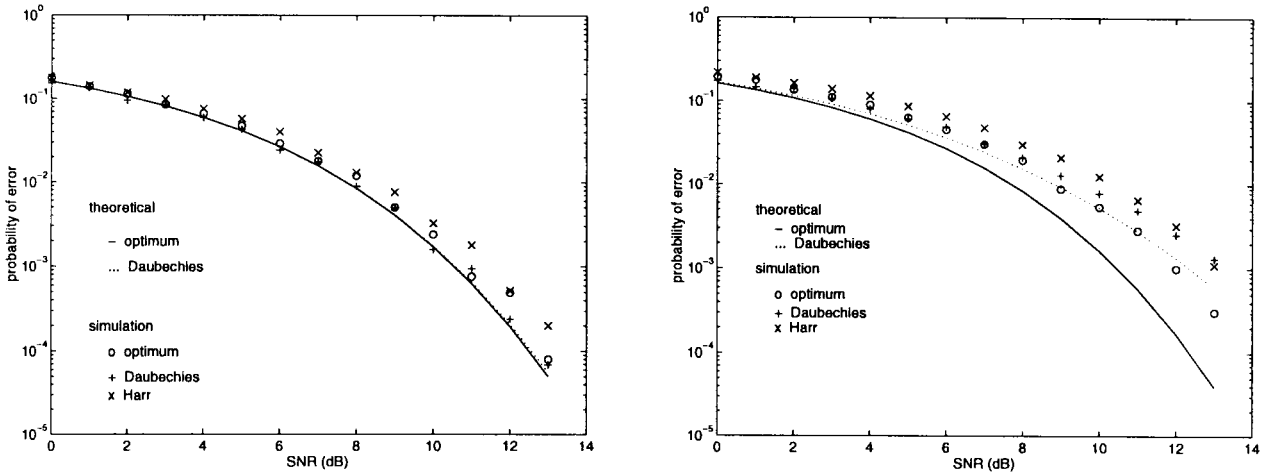

(a) (b)

Fig. 5. Probability of error for a range of SNR's for the two-channel scenario studied in Example 2.

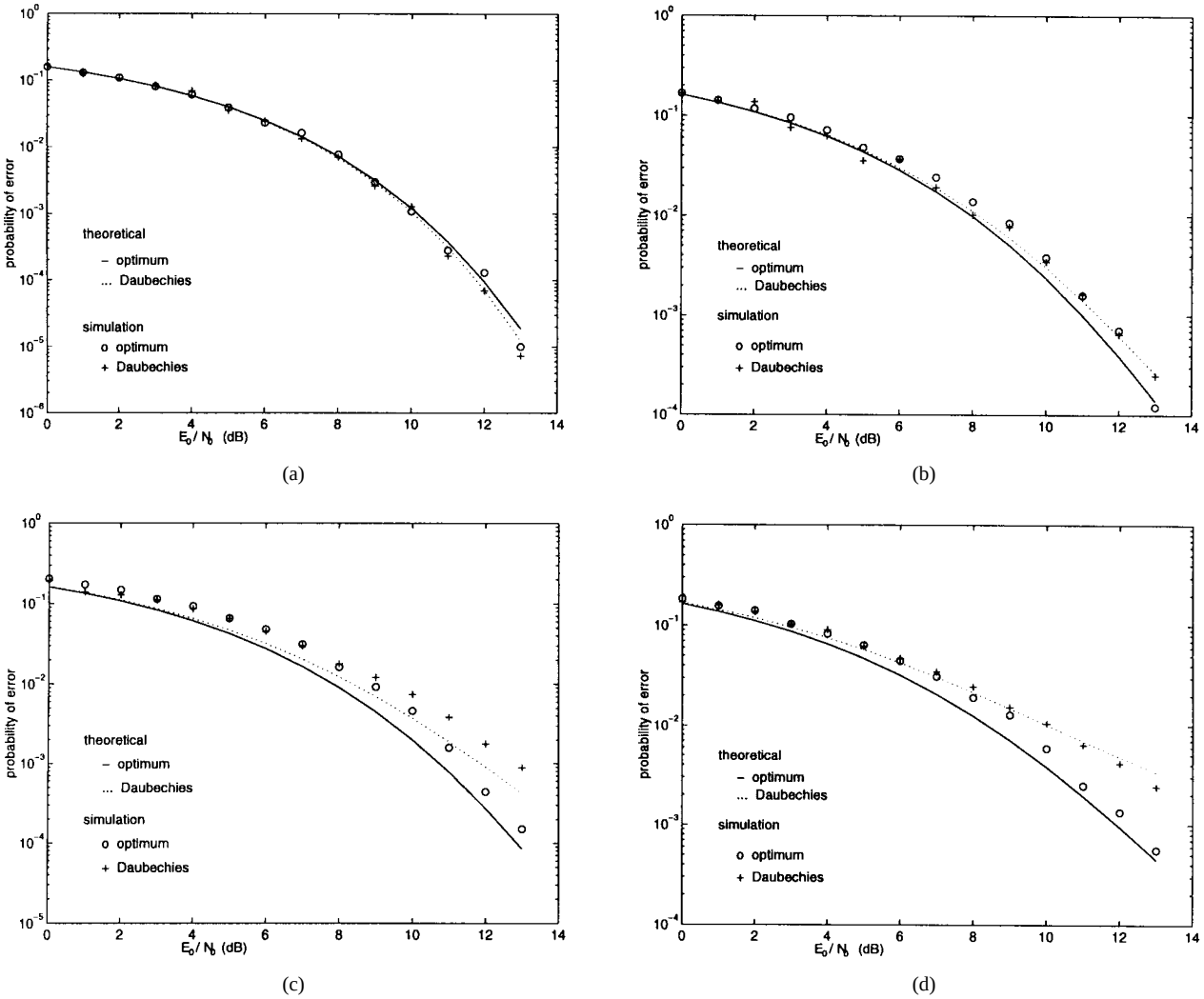

(a) (b)

(c) (d)

Fig. 6. Probability of error for a range of SNR's for the four channel scenario studied in Example 2.

the value of $I_{\ell m}[n]$ when the ith combination of ± 1 is substituted into $\sigma_{\lambda\mu}[j]$ in (23). We note that many of the $I_{\ell m;i}$ under different combinations of ± 1 are of equal value.

Now, let us consider the probability of decision error due to the combined effects of timing error interference and zero-mean white Gaussian channel noise having power spectral

density $S_\nu(\omega) = N_0/2$. The output noise of the correlator and sampler is a zero-mean Gaussian random variable with variance given by

$$\begin{aligned} E\{\nu_{\ell m}^2[n]\} &= \iint E\{\nu(t)\nu(\tau)\}\phi_{\ell m}(t - nT_\ell + \Delta)\phi_{\ell m} \\ &\quad \cdot (\tau - nT_\ell + \Delta)\, dt\, d\tau \\ &= \frac{N_0}{2}\iint \delta(t-\tau)\phi_{\ell m}(t - nT_\ell + \Delta) \\ &\quad \cdot \phi_{\ell m}(\tau - nT_\ell + \Delta)\, dt\, d\tau = N_0/2 \end{aligned}$$

where $E\{\cdot\}$ denotes expected value. In the presence of timing error, the expected value of the output of the (ℓ, m)th correlator when a "1" is transmitted at the (ℓ, m)th transmitter terminal is $1 + u_{\ell m}$. Therefore, the probability of error due to channel noise under the influence of timing error is

$$\begin{aligned} P_{\ell m}(\varepsilon|u_{\ell m}) &= \frac{1}{\sqrt{\pi N_0}}\int_{-\infty}^{0} \exp(-(\upsilon - (1+u_{\ell m}))^2/N_0)\, d\upsilon \\ &= \frac{1}{2}\,\mathrm{erfc}\left(\frac{1+u_{\ell m}}{\sqrt{N_0}}\right) \end{aligned} \tag{34}$$

where $\mathrm{erfc}(\alpha) = (2/\sqrt{\pi})\int_\alpha^\infty \exp(-z^2)\, dz$. Hence, the probability of error for the (ℓ, m)th terminal is given by

$$\begin{aligned} P_{\ell m}(\varepsilon) &= \int P_{\ell m}(\varepsilon|u_{\ell m})p(u_{\ell m})\, du_{\ell m} \\ &= \frac{1}{L_{\ell m}}\sum_{i=1}^{L_{\ell m}} \mathrm{erfc}\left(\frac{1+I_{\ell m;i}}{\sqrt{N_0}}\right) \end{aligned} \tag{35}$$

where (33) has been used in the second step.

Equation (35) yields an exact expression for the probability of decision error in the (ℓ, m)th terminal due to timing error and Gaussian noise. To use (35), the possible interference values $I_{\ell m;i}$ generated by all possible combinations of values of $\sigma_{\lambda\mu}$ filtered by $J_{\ell m}^{\lambda\mu}$ have to be evaluated. Unfortunately, $L_{\ell m}$ may be a large number (e.g., for $\ell = 2, M_\ell = 4$ and $N = 14, L_{\ell m} = 2^{316}$), which may make (35) difficult to apply. We can, however, approximate (35) using the central limit theorem [48]. Since the random variable $u_{\ell m}$ is a linear combination of a large number of binary random variables, we can approximate it by a random variable $\hat{u}_{\ell m}$ having a Gaussian PDF. Note that the mean of $u_{\ell m}$ is zero, and the maximum and minimum values of $u_{\ell m}$ occur when all $\sigma_{\lambda\mu}[j]$ in (23) are $+1$ and -1, respectively, with coefficients $|J_{\ell m}^{\lambda\mu}[n]|$. We may take these maximum and minimum values to be $\pm 3\zeta_{\ell m}$, where $\zeta_{\ell m}$ denotes the standard deviation of $\hat{u}_{\ell m}$. In this way, we have ensured that the probability of finding the approximated random variable $\hat{u}_{\ell m}$ within this range is over 99.7%. Substituting (34) and $p(\hat{u}_{\ell m})$ into (35), interchanging the order of integration, and factorizing the exponential part, the approximated probability of error can be written as

$$\begin{aligned} \hat{P}_{\ell m}(\varepsilon) &= \int_{-\infty}^{\infty} \frac{1}{\zeta_{\ell m}\sqrt{2\pi}}\, \exp(-\hat{u}_{\ell m}^2/(2\zeta_{\ell m}^2)) \int_{-\infty}^{0} \\ &\quad \cdot \frac{1}{\sqrt{\pi N_0}}\, \exp(-(\upsilon - (1+\hat{u}_{\ell m}))^2/N_0)\, d\upsilon\, d\hat{u}_{\ell m} \\ &= \frac{1}{2}\,\mathrm{erfc}(1/\sqrt{N_0 + 2\zeta_{\ell m}^2}). \end{aligned} \tag{36}$$

Equation (36) indicates that a smaller variance of interference $\zeta_{\ell m}^2$ leads to a smaller probability of error in the (ℓ, m)th terminal. The optimum scaling function design seeks to minimize the total energy of the interference, which may often lead to a lower expected value of $\zeta_{\ell m}$. Thus, we may expect the average probability of error over all the terminals using the optimum scaling function to be lower than that using other scaling functions. This is illustrated by the following example.

Example 2: Consider a WPDM system consisting of two branches, using $\phi_{11}(t - nT_1)$ and $\phi_{12}(t - nT_1)$ as carriers for the binary message signals $\sigma_{11}[n]$ and $\sigma_{12}[n]$. The transmission of the modulated signal through a communication channel is disrupted by spectrally white zero-mean Gaussian noise, the spectral density of which is $N_0/2$. At the receiver, the signal is demodulated by a correlator and sampler at the root of the WPDM tree, which has a timing error Δ relative to the transmitted carrier scaling function. The output of the correlator and sampler $\hat{\sigma}_{01}[n]$ is then passed through a wavelet packet decomposer to obtain the sequences $\hat{\sigma}_{11}[n]$ and $\hat{\sigma}_{12}[n]$.

The performance of such a system, in terms of the bit error rate under different signal-to-noise ratios (SNR), was evaluated both theoretically and by simulation. (Since the bit energy is normalized to unity, SNR $= 10\ \log_{10}(1/N_0)$ dB.) For a timing discrepancy of $\Delta = 0.15T_0$, the results obtained by employing the optimum scaling function designed in Example 1, the Daubechies scaling functions of the same duration, and the Haar scaling function (the well-known unit-energy full duty cycle rectangular pulse of duration T_0) are plotted in Fig. 5(a) and (b) for the the message signals at the (1,1) and (1,2) terminals, respectively.[2] The theoretical error rates given by (36) are also plotted for reference. It can be observed that for the message signal $\sigma_{11}[n]$, the performance of the WPDM scheme using the optimum scaling function $\tilde{\phi}_{01}(t)$ is almost identical to that obtained by the Daubechies function, both in simulation and theoretically, being slightly superior to the use of the Haar function. In addition, the theoretical analyses agree very well with the simulation results.

For the message $\sigma_{12}[n]$, the theoretical performance using $\tilde{\phi}_{01}(t)$ is almost the same as the corresponding performance for $\sigma_{11}[n]$, but the theoretical performance using Daubechies functions has greatly deteriorated. This can be easily explained by the difference in the amount of interference at the (1,2) terminal, as shown in Table III. With much higher interference, using the Daubechies function will certainly result in inferior performance. That the use of $\tilde{\phi}_{01}(t)$ results in superior performance to the Daubechies or Haar functions is also confirmed by the simulations. However, there is a discrepancy between the theoretical evaluation of performance and that from simulation in each case. The discrepancy can be attributed to the terms containing second and higher order powers of Δ being ignored in (17). The second and higher order terms in (17) contain second and higher order derivatives of $R_\phi(\tau)$ and, therefore, tend to have little or no low-frequency content. (Differentiation in the time domain is equivalent to

[2]For easier viewing of the graphs, the results obtained using the Lemarié–Battle scaling function (which are inferior to the Daubechies functions due to higher interference) are omitted. The theoretical values of $P_{\ell m}(\varepsilon)$ for the case of the Haar function cannot be evaluated using (36) because the autocorrelation function of the Haar function is not differentiable in the conventional sense.

multiplication by ω in the frequency domain.) These higher order terms are passed through a LP filter $h[n]$ and a HP filter $g[n]$ (just as the first-order terms are) to form parts of the interference at the (1,1) and (1,2) terminals, respectively. Due to the HP nature of these higher order interference terms, their contribution to the interference in the (1,2) terminal is much more significant than that to the (1,1) terminal. Thus, ignoring these terms in the linear approximation will lead to a larger discrepancy between the theoretical and simulated results at the (1,2) terminal than at the (1,1) terminal. In Fig. 5(b), the difference in performance between using the optimum scaling function $\tilde{\phi}_{01}(t)$ and the Daubechies function become significant only when the SNR is relatively high (≥ 8 dB). This is because at low SNR, the performance is dominated by errors due to the Gaussian channel noise.

Fig. 6(a)–(d) show a comparison of the performance of a second-level $(\ell = 2, M_2 = 4)$ WPDM tree structure using the constituent terminal functions of the optimum scaling function $\tilde{\phi}_{01}(t)$ and the corresponding Daubechies function. [The theoretical performance is evaluated using (36).] Again, at the first two terminals, i.e., the (2,1) and (2,2) terminals, the difference between the performance of the optimal and Daubechies schemes are rather small. However, at the (2,3) and (2,4) terminals, the use of the constituent terminal functions of $\tilde{\phi}_{01}(t)$ results in superior performance to the use of the constituent terminal functions of the Daubechies scaling function.

VI. Conclusion

In this paper, a new scheme for transmitting multiple signals using wavelet packets (WPDM) has been proposed. The concepts of the scheme were outlined, and the transmission and reception systems, with their equivalent realizations, were developed. Wavelet packet basis functions are employed as coding waveforms because they provide self orthogonality based on time translation and mutual orthogonality based on occupancy of different orthogonal subspaces (although, of course, such functions are not the only class of functions providing such properties). Such orthogonalities allow the waveforms to be overlapped in both time and frequency, eliminating the need for guard bands, as in FDM, or for guard times, as in TDM, and thereby increasing the capacity of the transmission channel. In addition, the transmission system also offers communication security since knowledge of the choice of wavelet packet is required for decoding of the message signals. While WPDM offers these advantages, we note that in common with several other communication schemes (e.g., rectangular 16-QAM), the transmitted signal does not have a constant envelope. In order to control the effects of envelope variations, we may have to limit the transmission power in order to avoid operating the transmission amplifiers near their nonlinear saturation regions [5]. If an attempt is made to restore the constant envelope characteristic by passing the composite signal through a hard limiter, the orthogonality of the constituent terminal functions may be destroyed, resulting in potentially unacceptable performance.

We have examined the problem of timing error in WPDM and observed that the interference due to a timing discrepancy between the transmitter and receiver is made up of two components (intersymbol interference and crosstalk), which can be, respectively, modeled as the message bits from the given channel and the adjacent channels passed through corresponding (multirate) filters. These simple models led us to propose an optimum design of the coding waveforms (i.e., the scaling function and its constituents) in which the total timing-error interference is minimized. We also obtained expressions for the probability of error under the effects of timing error and additive white Gaussian channel noise. Simulations confirmed these expressions and showed that employing the optimum scaling function results in a lower probability of error in transmission than other commonly used scaling functions.

In this paper, we have focused our attention on orthogonal multiple signal transmission. We can easily obtain extra degrees of freedom by expanding our formulation to biorthogonal signaling using biorthogonal wavelet packets and filter banks [39], [49]. However, we note that Proposition 1 no longer holds, and the minimization of the total interference energy becomes structure dependent. We must therefore reformulate the optimization in terms of the interference energies at each level. Furthermore, care must be taken in order to avoid excessive noise gain and numerical instability [50] in the wavelet packet decomposer.

In continuing work [51], [52], we have shown that the (orthogonal) WPDM system performs better than the TDM system under impulsive noise and better than the FDM system in certain fading environments. Given the ever-increasing demand on channel capacity in communication systems, the capacity advantages of WPDM, together with the simplicity of its implementation and its emerging robustness properties, show that WPDM holds considerable promise as a multiple signal transmission technique.

References

[1] B. Sklar, *Digital Communications. Fundamentals and Applications*. Englewood Cliffs, NJ: Prentice-Hall, 1988.

[2] L. E. Franks, *Signal Theory*. Englewood Cliffs, NJ: Prentice-Hall, 1969.

[3] S. Haykin, *Communication Systems*, 3rd ed. New York: Wiley, 1994.

[4] J. G. Proakis, *Digital Communications*, 3rd ed. New York: McGraw-Hill, 1995.

[5] E. A. Lee and D. G. Messerschmitt, *Digital Communications*, 2nd ed. Boston, MA: Kluwer, 1993.

[6] G. W. Wornell and A. V. Oppenheim, "Wavelet-based representations of self-similar signals with application to fractal modulation," *IEEE Trans. Inform. Theory (Special Issue on Wavelet Transforms and Multiresolution Signal Analysis)*, vol. 38, pt. II, pp. 785–800, Mar. 1992.

[7] D. Cochran and C. Wei, "Scale based coding of digital communication signals," in *Proc. IEEE-SP Int. Symp. Time-Frequency and Time-Scale Anal.*, Oct. 1992, pp. 455–458.

[8] M. A. Tzannes and M. C. Tzannes, "Bit-by-bit channel coding using wavelets," in *Proc. IEEE Global Telecommun. Conf.*, 1992, pp. 684–688.

[9] P. P. Ghandi, S. S. Rao, and R. S. Pappu, "On waveform coding using wavelets," in *Proc. 27th Asilomar Conf. Signals, Syst., Comput.*, Pacific Grove, CA, 1993, pp. 901–905.

[10] R. E. Learned, H. Krim, B. Claus, A. S. Willsky, and W. C. Karl, "Wavelet-packet-based multiple access communication," in *Wavelet Applications in Signal and Image Processing II*, A. F. Laine and M. A. Unser, Eds., vol. 2303 of *Proc. SPIE*, pp. 246–259, Oct. 1994.

[11] S. D. Sandberg and M. A. Tzannes, "Overlapped discrete multitone modulation for high speed copper wire communications," *IEEE J. Select. Areas Commun.*, vol. 13, pp. 1571–1585, Dec. 1995.

[12] K. Hetling, G. J. Saulnier, and P. K. Das, "Optimized perfect reconstruction quadrature mirror filter (PR-QMF) based codes for multi-user

communications," in *Wavelet Applications II*, vol. 2491 of *Proc. SPIE*, Apr. 1995, pp. 248–259.
[13] R. S. Orr, C. Pike, and M. J. Lyall, "Wavelet transform domain communication systems," in *Wavelet Applications II*, vol. 2491 of *Proc. SPIE*, Apr. 1995, pp. 271–282.
[14] A. R. Lindsey, "Multi-dimensional signaling via wavelet packets," in *Wavelet Applications II*, vol. 2491 of *Proc. SPIE*, Apr. 1995, pp. 303–314.
[15] J. Wu, Q. Jin, and K. M. Wong, "Multiplexing based on wavelet packets," in *Wavelet Applications II*, vol. 2491 of *Proc. SPIE*, Apr. 1995, pp. 315–326.
[16] G. W. Wornell, "Emerging applications of multirate signal processing and wavelets in digital communications," *Proc. IEEE (Special Issue on Wavelets)*, vol. 84, pp. 586–603, Apr. 1996.
[17] Y. Meyer, *Ondelettes*, vol. 1 of *Ondelettes et opérateurs*. Paris, France: Hermann, 1990, in French; Y. Meyer, *Wavelets and Operators*. Cambridge, U.K.: Cambridge Univ. Press, 1992, English translation by D. H. Salinger.
[18] I. Daubechies, *Ten Lectures on Wavelets*. Philadelphia, PA: SIAM, 1992.
[19] C. K. Chui, *An Introduction to Wavelets*. Boston, MA: Academic, 1992.
[20] A. N. Akansu and R. A. Haddad, *Multiresolution Signal Decomposition. Transforms, Subbands, and Wavelets*. Boston, MA: Academic, 1992.
[21] P. P. Vaidyanathan, *Multirate Systems and Filter Banks*. Englewood Cliffs, NJ: Prentice-Hall, 1993.
[22] G. G. Walter, *Wavelets and Other Orthogonal Systems with Applications*. Boca Raton, FL: CRC, 1994.
[23] M. Vetterli and J. Kovačević, *Wavelets and Subband Coding*. Englewood Cliffs, NJ: Prentice-Hall, 1995.
[24] G. Strang and T. Q. Nguyen, *Wavelets and Filter Banks*. Wellesley, MA: Wellesley-Cambridge Univ. Press, 1996.
[25] G. Strang, "Wavelets and dilation equations: A brief introduction," *SIAM Rev.*, vol. 31, pp. 614–627, Dec. 1989.
[26] O. Rioul and M. Vetterli, "Wavelets and signal processing," *IEEE Signal Processing Mag.*, vol. 8, pp. 14–38, Oct. 1991.
[27] B. Jawerth and W. Sweldens, "An overview of wavelet based multiresolution analysis," *SIAM Rev.*, vol. 36, pp. 377–412, Sept. 1994.
[28] A. Cohen and J. Kovačević, "Wavelets: The mathematical background," *Proc. IEEE (Special Issue on Wavelets)*, vol. 84, pp. 514–522, Apr. 1996.
[29] N. Hess-Nielsen and M. V. Wickerhauser, "Wavelets and time-frequency analysis," *Proc. IEEE (Special Issue on Wavelets)*, vol. 84, pp. 523–540, Apr. 1996.
[30] K. Ramchandran, M. Vetterli, and C. Herley, "Wavelets, subband coding, and best bases," *Proc. IEEE (Special Issue on Wavelets)*, vol. 84, pp. 541–560, Apr. 1996.
[31] S. G. Mallat, "A theory for multiresolution signal decomposition: The wavelet transform," *IEEE Trans. Pattern Anal. Machine Intell.*, vol. 11, pp. 674–693, July 1989.
[32] I. Daubechies, "Orthonormal bases of compactly supported wavelets," *Commun. Pure Applied Math.*, vol. XLI, no. 7, pp. 909–996, Oct. 1988.
[33] A. V. Oppenheim, A. S. Willsky, with I. T. Young, *Signals and Systems*. Englewood Cliffs, NJ: Prentice-Hall, 1983.
[34] R. R. Coifman and M. V. Wickerhauser, "Entropy-based algorithms for best basis selection," *IEEE Trans. Inform. Theory (Special Issue on Wavelet Transforms and Multiresolution Signal Analysis)*, vol. 38, pt. 2, pp. 713–718, Feb. 1992.
[35] C. E. Sundberg, "Continuous phase modulation: A class of jointly power and bandwidth efficient modulation scheme with constant amplitude," *IEEE Commun. Mag.*, vol. 24, pp. 25–38, Apr. 1986.
[36] L. E. Franks, "Carrier and bit synchronization in data communication—A tutorial review," *IEEE Trans. Commun.*, vol. COM–28, pp. 1107–1121, Aug. 1980.
[37] W. Kaplan, *Advanced Calculus*. Reading, MA: Addison-Wesley, 1952.
[38] N. Saito and G. Beylkin, "Multiresolution representations using the autocorrelation functions of compactly supported wavelets," *IEEE Trans. Signal Processing (Special Issue on Wavelets and Signal Processing)*, vol. 41, pp. 3584–3590, Dec. 1993.
[39] M. Vetterli and C. Herley, "Wavelets and filter banks: Theory and design," *IEEE Trans. Signal Processing*, vol. 40, pp. 2207–2232, Sept. 1992.
[40] J. Wu, "Wavelet packet division multiplexing," Ph.D. dissertation, Dept. Elect. Comput. Eng., McMaster Univ., Hamilton, Ont., Canada, 1997.
[41] I. Daubechies, "Orthonormal bases of compactly supported wavelets II. Variations on a theme," *SIAM J. Math. Anal.*, vol. 24, no. 2, pp. 499–519, Mar. 1993.
[42] P. E. Gill, W. Murray, and M. H. Wright, *Practical Optimization*. London, U.K.: Academic, 1981.
[43] B. P. Lathi, *Modern Digital and Analog Communication Systems*, 2nd ed. New York: HRW, 1989.
[44] C. K. Campbell, *Surface Acoustic Wave Devices and their Signal Processing Applications*. New York: Academic, 1989.
[45] R. Kellejian, *Applied Electronic Communication*. New York: SRA, 1980.
[46] P. G. Lemarié, "Ondelettes à localization exponentielle," *J. Mathématiques Pures et Appliquèes*, vol. 67, no. 3, pp. 227–236, 1988.
[47] G. Battle, "A block spin construction of ondelettes. Part I: Lemarié functions," *Commun. Math. Phys.*, vol. 110, no. 4, pp. 601–615, 1987.
[48] A. Leon-Garcia, *Probability and Random Processes for Electrical Engineering*, 2nd ed. Reading, MA: Addison-Wesley, 1994.
[49] A. Cohen, I. Daubechies, and J. C. Feauveau, "Biorthogonal bases of compactly supported wavelets," *Commun. Pure Applied Math.*, vol. XLV, no. 5, pp. 485–560, June 1992.
[50] A. Cohen and I. Daubechies, "On the instability of arbitrary biorthogonal wavelet packets," *SIAM J. Math. Anal.*, vol. 24, no. 5, pp. 1340–1354, Sept. 1993.
[51] J. Wu, K. M. Wong, Q. Jin, and T. N. Davidson, "Performance of wavelet packet division multiplexing in impulsive and Gaussian noise channels," in *Wavelet Applications in Signal and Image Processing IV*, M. A. Unser, A. Aldroubi, and A. F. Laine, Eds., vol. 2825 of *Proc. SPIE*, pp. 516–527, Oct. 1996.
[52] J. Wu, K. M. Wong, and Q. Jin, "Performance of wavelet packet division multiplexing in timing errors and flat fading channels," in *Proc. 3rd Int. Workshop Image Signal Process.*, B. G. Mertzios and P. Liatsis, Eds., Manchester, U.K., Nov. 1996, pp. 381–384..
[53] H. H. Szu, Ed., *Wavelet Applications II*, vol. 2491 of *Proc. SPIE*, Apr. 1995.

Kon Max Wong (SM'81) was born in Macau. He received the B.Sc.(Eng), DIC, Ph.D., and D.Sc.(Eng) degrees, all in electrical engineering, from the University of London, U.K., in 1969, 1972, 1974, and 1995, respectively.

He started working at the Transmission Division of Plessey Telecommunications Research Ltd., London, in 1969. In October 1970, he was on leave from Plessey, pursuing postgraduate studies and research at Imperial College of Science and Technology, London. In 1972, he rejoined Plessey as a research engineer and worked on digital signal processing and signal transmission. In 1976, he joined the Department of Electrical Engineering, Technical University of Nova Scotia, Halifax, N.S., Canada, and in 1981, he moved to McMaster University, Hamilton, Ont., Canada, where he has been a Professor and Chairman of the Department of Electrical and Computer Engineering. He is currently on leave at the Department of Electronic Engineering, Chinese University of Hong Kong. His research interest is in the area of signal processing and communication theory.

Prof. Wong is the recipient of the IEE Overseas Premium in 1989 and is a Fellow of the Institution of Electrical Engineers, a Fellow of the Royal Statistical Society, and a Fellow of the Institute of Physics.

Jiangfeng Wu received the B.S. and M.S. degrees in electrical engineering from Beijing University of Aeronautics and Astronautics, Beijing, China, in 1987 and 1990, respectively. Since January 1994, she has been in the Ph.D. program with the Department of Electrical and Computer Engineering, McMaster University, Hamilton, Ont., Canada. Her thesis is on the application of wavelets and wavelet packets in modulation and multiplexing.

b From 1990 to 1993, she was a Lecturer with the Department of Electrical Engineering, Beijing University of Aeronautics and Astronautics. She worked as a software engineer with Telexis Corporation, Ottawa, Ont., from August 1996 to March 1997. Since April 1997, she has been a digital signal processing engineer in the Wireless Networks Division of Nortel, Ottawa. Her research interests include wireless communication systems, fading channels, modulation schemes, digital signal processing, and the application of wavelets and wavelet packets in telecommunications.

Tim N. Davidson (M'96) received the B.E. (Hons. I) degree in electronic engineering from The University of Western Australia (UWA), Perth, in 1991 and the D.Phil. degree in engineering science from the The University of Oxford, Oxford, U.K., in 1995.

He is a post-doctoral research fellow and a part-time lecturer at the Communications Research Laboratory, McMaster University, Hamilton, Ont., Canada. His research interests are in signal processing and control, with current activity focussed on signal processing applications in digital communication systems. He has held research positions at the Adaptive Signal Processing Laboratory at UWA and the Australian Telecommunications Research Institute, Curtin University of Technology, Brisbane, Australia, and brief visiting appointments at QPSX Communications and the Digital Signal Processing Laboratory at The Chinese University of Hong Kong. He has also held project engineering positions at several mine sites in Western Australia.

Dr. Davidson was awarded the 1991 J. A. Wood Memorial Prize for "the most outstanding [UWA] graduate" in the pure and applied sciences and the 1991 Rhodes Scholarship for Western Australia.

Qu (Gary) Jin received the B.Eng. and M.Eng. degrees from Dalian Maritime University, Dalian, China, in 1982 and 1985, respectively, and Ph.D. degree from McMaster University, Hamilton, Ont., Canada, in 1992.

From 1985 to 1986, he was employed as a Lecturer in the Department of Electronic Engineering, Dalian Maritime University. From September 1986 to September 1987, he was a Visiting Scholar with the Department of Electrical and Computer Engineering, McMaster University. In 1991, he worked worked in the Communication Research Laboratory, McMaster University, as a Post-Doctoral Fellow and later as a Research Engineer. He was also an Adjunct Assistant Professor with the Department of Electrical and Computer Engineering. In 1995, he joined Mitel Corporation, Kanata, Ont., Canada, where he is currently a Senior Integrated Circuit Design Engineer. His research interest is in the general area of digital signal processing and communications.